

Photoluminescence Properties and Spectral Structure Analysis of $\text{NaLn}(\text{MoO}_4)_2:\text{Eu}^{3+}$ ($\text{Ln} = \text{Gd}, \text{Y}$) Phosphors

Zuoling Fu^{1,*}, Xiaojie Wang¹, Tianqi Sheng¹, Xihong Fu², and Jung Hyun Jeong^{3,*}

¹State Key Laboratory of Superhard Materials, College of Physics, Jilin University, Changchun 130012, China

²Changchun Institute of Optics, Fine Mechanics and Physics, Chinese Academy of Sciences, Changchun 130033, China

³Department of Physics, Pukyong National University, Busan 608-737, South Korea

In this paper, a facile synthetic route for the preparation of $\text{NaLn}(\text{MoO}_4)_2:\text{Eu}^{3+}$ ($\text{Ln} = \text{Gd}, \text{Y}$) nanocrystals by a hydrothermal method is reported. The $\text{NaLn}(\text{MoO}_4)_2:\text{Eu}^{3+}$ ($\text{Ln} = \text{Gd}, \text{Y}$) micro-powders were synthesized by a high temperature solid-state reaction. The optical properties of Eu^{3+} as a local structural probe are analyzed when being incorporated into $\text{NaLn}(\text{MoO}_4)_2$ ($\text{Ln} = \text{Gd}, \text{Y}$) micro-powders and nanocrystals. In $\text{NaLn}(\text{MoO}_4)_2:\text{Eu}^{3+}$ ($\text{Ln} = \text{Gd}, \text{Y}$), the substitution of Ln^{3+} by Eu^{3+} is confirmed and the point symmetry of the site and crystal structure are analyzed. The luminescence mechanism and the size dependence of their fluorescence properties in $\text{NaLn}(\text{MoO}_4)_2:\text{Eu}^{3+}$ ($\text{Ln} = \text{Gd}, \text{Y}$) micro-powders and nanocrystals are also discussed in detail.

Keywords: Photoluminescence Properties, Site-Selective Spectroscopy, $\text{NaLn}(\text{MoO}_4)_2:\text{Eu}^{3+}$ ($\text{Ln} = \text{Gd}, \text{Y}$) Phosphors.

1. INTRODUCTION

The rare earth-molybdenum (VI) oxides system constitutes a very rich family within which a great variety of compounds can be synthesized with different stoichiometry and structure. Recently, many works focused on luminescence properties research of molybdates doped with rare earth ions also have been carried out^{1–7} because molybdates have been widely used as host candidates for white light-emitting diodes (LEDs). The optical properties of molybdates are structure-dependent. In addition, molybdates can exist in different valences of the molybdenum element. The formation of different phase structures depends on the preparation approach, reaction temperature, the pH value of the reaction system, and the stoichiometric ratio of starting materials.

$\text{MLn}(\text{MoO}_4)_2$ ($\text{M} = \text{alkali metal}$, $\text{Ln} = \text{rare earth}$) molybdate crystals are attractive host materials, not only because of their large lanthanide admittance, but especially owing to their good optical properties.^{8–11} In the fields of phosphor materials, Eu or Tb doped $\text{MLn}(\text{MoO}_4)_2$ compounds present excellent luminescent properties.^{2,12} In Wang et al.'s¹² reports, it is interesting that no concentration quenching of Eu can be observed in the samples

of $\text{NaLn}_{1-x}\text{Eu}_x(\text{MoO}_4)_2$ and $\text{LiEu}(\text{MoO}_4)_2$ systems, both of which exhibit the strongest red emission under 395 nm light excitation and appropriate CIE chromaticity coordinates (0.66, 0.34) close to the NTSC standard values.

Not only the research on the optical properties of scheelite-type $\text{MLn}(\text{MoO}_4)_2$ is the hot topic, but also the research on their microstructure attracts much attention.^{13,14} The scheelite-type $\text{MLn}(\text{MoO}_4)_2$ is a tetragonal phase with a space group symmetry of $I4_1/a$ (C_{4h}^6). The double molybdates such as $\text{MLn}(\text{MoO}_4)_2$ ($\text{M} = \text{Na}$) show the scheelite-type structure for all rare-earth elements. In this structure, Mo^{6+} is coordinated by four oxygen atoms in a tetrahedral site, and the Ln^{3+} ions are located in the oxygen polyhedron in the form of LnO_8 units with an eight-coordination number. Generally, Eu^{3+} luminescence is of special importance as a spectral probe from its applications in phosphor materials. This is possible for the reason that Eu^{3+} has several structure-dependent transitions enabling one to gain insight about the site that occupies in a given host. Most of the previous works about rare earth molybdate compounds are mainly concentrated on the material synthesis and luminescence, and little has been done on the luminescence of the europium dependence of the molybdate crystal structure. On this basis, we have attempted to explore the different cationic sites present in the molybdates system.

*Authors to whom correspondence should be addressed.

In this work, $\text{NaLn}(\text{MoO}_4)_2\text{:Eu}^{3+}$ ($\text{Ln} = \text{Gd}, \text{Y}$) nanocrystalline and micro-powders were synthesized by a hydrothermal method and high temperature solid-state reaction, respectively. The site-selective excitation and emission spectra have been investigated under the pulsed dye-laser excitation in the ${}^5\text{D}_0\text{--}{}^7\text{F}_0$ region of Eu^{3+} in $\text{NaLn}(\text{MoO}_4)_2$ ($\text{Ln} = \text{Gd}, \text{Y}$). Luminescence excitation and emission spectra were also applied to investigate their optical properties. The obtained results revealed that Eu^{3+} normally occupied in one crystallographic site in $\text{NaLn}(\text{MoO}_4)_2$ ($\text{Ln} = \text{Gd}, \text{Y}$) which was characterized and discussed.

2. EXPERIMENTAL DETAILS

2.1. Hydrothermal Synthesis of Eu^{3+} Doped Nanocrystal $\text{NaLn}(\text{MoO}_4)_2$ ($\text{Ln} = \text{Gd}, \text{Y}$) Phosphors

In this paper, nanocrystalline $\text{NaGd}(\text{MoO}_4)_2\text{:2\%Eu}^{3+}$ powders were prepared by a hydrothermal method. $\text{Gd}(\text{NO}_3)_3 \cdot 6\text{H}_2\text{O}$ (analytical reagent, AR) and $\text{Eu}(\text{NO}_3)_3 \cdot 5\text{H}_2\text{O}$ (AR) were dissolved in 25 ml of distilled water and the mixture was stirred for 1 h. $(\text{NH}_4)_6\text{Mo}_7\text{O}_{24} \cdot 4\text{H}_2\text{O}$ (AR) was dissolved in another 25 ml of distilled water. After being completely dissolved, $(\text{NH}_4)_6\text{Mo}_7\text{O}_{24} \cdot 4\text{H}_2\text{O}$ was added to the previous solution and the pH value of the solution was adjusted to 6–7 by 5 M NaOH solution, and then stirred again for 2 h. The final mixture was transferred into a Teflon-lined stainless steel autoclave of 80 ml capacity and then sealed. The autoclave was maintained at 180 °C for 12 h and cooled naturally to room temperature. The precipitate was filtered and washed with alcohol and deionized water several times. Finally, the product was dried at 50 °C for 24 h. Finally, the pure phase $\text{NaGd}(\text{MoO}_4)_2\text{:2\%Eu}^{3+}$ nanocrystals were obtained.

For the $\text{NaY}(\text{MoO}_4)_2\text{:Eu}^{3+}$ nanocrystals, the detailed hydrothermal procedure is similar to Eu^{3+} -doped nanocrystal $\text{NaGd}(\text{MoO}_4)_2$. However, further calcinations is necessary, and the as-prepared sample were retrieved through a heat treatment at 800 °C in air for 4 h and then slowly cooled to room temperature. Finally, the pure phase $\text{NaY}(\text{MoO}_4)_2\text{:2\%Eu}^{3+}$ nanocrystals were obtained.

2.2. Preparation of Eu^{3+} Doped $\text{NaLn}(\text{MoO}_4)_2$ ($\text{Ln} = \text{Gd}, \text{Y}$) Micro-Powder Phosphors

The Eu^{3+} doped $\text{NaLn}(\text{MoO}_4)_2$ ($\text{Ln} = \text{Gd}, \text{Y}$) micro-powder crystals were prepared by using the high temperature solid-state reaction technique. The starting materials were $\text{Na}_2\text{CO}_3 \cdot \text{H}_2\text{O}$ (analytical reagent, AR), Gd_2O_3 (99.99%), Y_2O_3 (99.99%), Eu_2O_3 (99.99%), and $(\text{NH}_4)_6\text{Mo}_7\text{O}_{24} \cdot 4\text{H}_2\text{O}$ (analytical reagent, AR). According to the nominal compositions of $\text{NaGd}(\text{MoO}_4)_2\text{:2\%Eu}$ compounds, the appropriate amount of starting materials was thoroughly mixed and ground, then heated at 500 °C for 2 h. After being reground, they were calcined at 900 °C for 4 h in air. The $\text{NaGd}(\text{MoO}_4)_2\text{:2\%Eu}$ micro-powders

were obtained. For $\text{NaY}(\text{MoO}_4)_2\text{:2\%Eu}$ micro-powders, the detailed procedure is similar to that for preparing Eu^{3+} -doped $\text{NaGd}(\text{MoO}_4)_2$ micro-powders.

2.3. Characterization

The structural characteristics of the product were measured by the X-ray diffraction (XRD) using a Philips XPert/MPD diffraction system with $\text{Cu K}\alpha$ ($\lambda = 0.15405 \text{ nm}$) radiation. The morphology and size of the obtained samples were observed with field emission-scanning electron microscopy (FE-SEM, JSM-6700F, JEOL). For the optical investigation, the ultraviolet-visible photoluminescence (PL) excitation and emission spectra were recorded with a spectrophotometer (Hitachi F-7000) equipped with Xe-lamp as an excitation source. The laser-selective excitation experiment and high-resolution emission spectra were achieved by means of a Rhodamin 6G tunable dye laser (Sirah Cobra-Stretch), which was pumped by a frequency-tripled 355 nm Nd:YAG laser (Spectra-Physics Quanta-Ray Pro-Series) with a 10 Hz repetition and a 10 ns pulse duration. The laser-induced fluorescence was collected by a lens ($f = 15 \text{ cm}$), filtered by a 0.5 m mono-chromator, and finally detected by a photomultiplier tube (Hamamatsu R3896). The intensity response of the detection system to the fluorescence signals at different wavelengths was calibrated by a standard lamp. The time-resolved fluorescence decay signals from the detector were recorded by a digital oscilloscope (LeCroy 9410) and processed with a boxcar integrator (Stanford Research Systems SR250). All the measurements were performed at room temperature.

3. RESULTS AND DISCUSSION

3.1. Crystal Structure and Morphology of Eu^{3+} Doped $\text{NaLn}(\text{MoO}_4)_2$ ($\text{Ln} = \text{Gd}, \text{Y}$) Micro-Powders and Nanocrystal Phosphors

Figure 1(a) shows the XRD patterns of $\text{NaGd}(\text{MoO}_4)_2\text{:Eu}^{3+}$ micro-powders and nanocrystalline in which all of the peaks could be indexed to the tetragonal phase of $\text{NaGd}(\text{MoO}_4)_2$ (JCPDS No. 25-0828). In $\text{NaGd}(\text{MoO}_4)_2\text{:Eu}^{3+}$ micro-powders the XRD pattern shows sharp diffraction features. However, the $\text{NaGd}(\text{MoO}_4)_2\text{:Eu}^{3+}$ nanocrystalline gives much broader and less intense peaks. The XRD patterns for $\text{NaY}(\text{MoO}_4)_2\text{:Eu}^{3+}$ micro-powders and nanocrystalline were shown in Figure 1(b), in which all of the peaks could be indexed to the tetragonal phase of $\text{NaY}(\text{MoO}_4)_2$ (JCPDS No. 52-1802). We have also performed the FE-SEM measurement on the $\text{NaGd}(\text{MoO}_4)_2$ and $\text{NaY}(\text{MoO}_4)_2$ micro-powders and nanocrystalline, as shown in Figures 2(a)–(d), respectively. The estimated average crystallite size is approximately 100 nm in $\text{NaGd}(\text{MoO}_4)_2\text{:Eu}^{3+}$ samples (Fig. 2(a)), while it is about 200 nm in $\text{NaY}(\text{MoO}_4)_2\text{:Eu}^{3+}$ samples with regular distribution (Fig. 2(c)). When the samples were prepared by the solid-state reaction, the particle grew up to about 5 μm

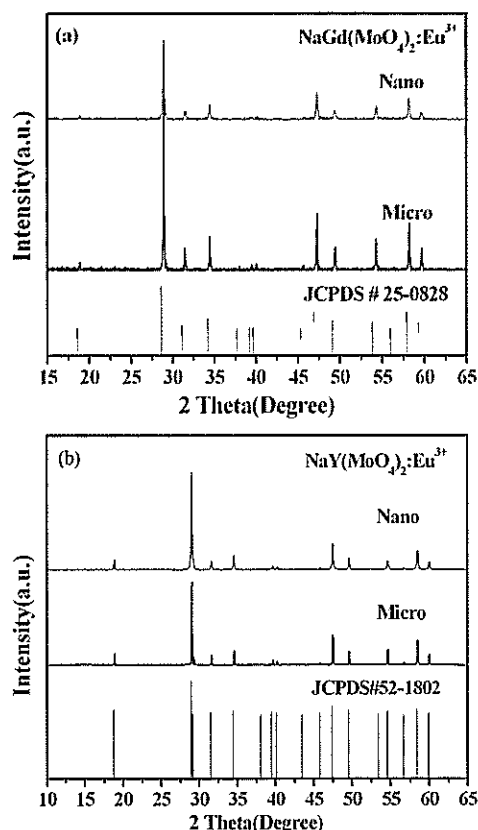


Figure 1. X-ray diffraction (XRD) patterns of micro-powders and nanocrystal $\text{NaGd}(\text{MoO}_4)_2:\text{Eu}^{3+}$ (a) and $\text{NaY}(\text{MoO}_4)_2:\text{Eu}^{3+}$ (b).

and joined together because of the elevated annealing temperature (Figs. 2(b) and (d)).

3.2. Photoluminescence (PL) and Excitation Spectra (PLE) of Eu^{3+} Doped $\text{NaLn}(\text{MoO}_4)_2$ ($\text{Ln} = \text{Gd}, \text{Y}$) Micro-Powders and Nanocrystal Phosphors

The PL and PLE spectra of Eu^{3+} doped $\text{NaLn}(\text{MoO}_4)_2$ ($\text{Ln} = \text{Gd}, \text{Y}$) micro-powders and nanocrystal were shown in Figures 3(a) and (b), indicating that the shapes of the photoluminescence of phosphors are similar. The excitation spectra (Fig. 3, left) were obtained by monitoring the emission of the $\text{Eu}^{3+} {}^5\text{D}_0\text{--}{}^7\text{F}_2$ transition at 616 nm. It can be observed clearly that the excitation spectra both consist of a broad band from 200 to 350 nm, which is ascribed to the O—Mo charge-transfer (CT) transition. The charge transfer band of O— Eu^{3+} , which usually appears in the range 250–300 nm in the excitation spectrum,⁹ might have overlapped with the CT band of molybdate group and hence not observed clearly. In the longer wavelength region (360–500 nm), the sharp lines are intraconfigurational $4f\text{--}4f$ transitions of Eu^{3+} in the host lattices, and the strong excitation bands at 395 and 466 nm are attributed to the ${}^7\text{F}_0\text{--}{}^5\text{L}_6$ and ${}^7\text{F}_0\text{--}{}^5\text{D}_2$ transitions of Eu^{3+} , respectively, which are matched well with nUV (350–410 nm) and blue (450–470 nm) LED chip. Both spectra (Figs. 3(a) and (b)) exhibit similar

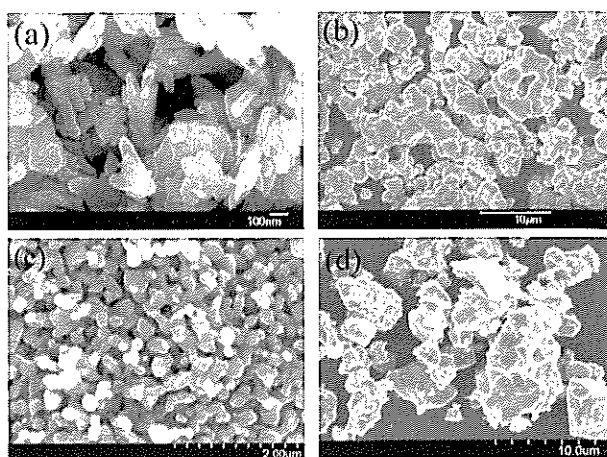


Figure 2. FE-SEM images of (a) $\text{NaGd}(\text{MoO}_4)_2:\text{Eu}^{3+}$ nanocrystals, (b) $\text{NaGd}(\text{MoO}_4)_2:\text{Eu}^{3+}$ micro-powders, (c) $\text{NaY}(\text{MoO}_4)_2:\text{Eu}^{3+}$ nanocrystals and (d) $\text{NaY}(\text{MoO}_4)_2:\text{Eu}^{3+}$ micro-powders.

profiles except for two specific features: (a) The spectrum of nanocrystalline $\text{NaGd}(\text{MoO}_4)_2:\text{Eu}^{3+}$ phosphor shows a high-intensity broad band with a maximum at ~ 292 nm, indicating that 292 nm may become good excitation light

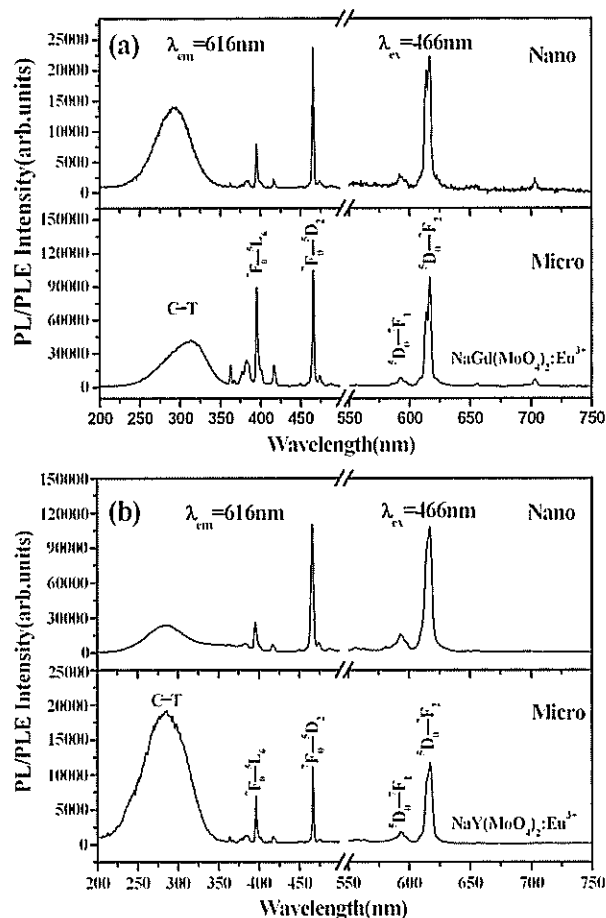


Figure 3. The excitation (left, $\lambda_{\text{em}} = 616$ nm) and emission (right, (a) $\lambda_{\text{ex}} = 395$ nm; (b) $\lambda_{\text{ex}} = 466$ nm) spectra of (a) $\text{NaGd}(\text{MoO}_4)_2:\text{Eu}^{3+}$ micro-powders and (b) $\text{NaY}(\text{MoO}_4)_2:\text{Eu}^{3+}$ nanocrystal phosphors.

to obtain strong intensity red emission as well as the 466 nm. One also reported that the energy absorbed by the MoO_4^{2-} group can be transferred to Eu^{3+} ions efficiently in $\text{La}_2(\text{MoO}_4)_3:\text{Eu}^{3+}$ phosphor. For the $\text{NaGd}(\text{MoO}_4)_2:\text{Eu}^{3+}$ micro-powder phosphor, its charge transfer band from O—Mo with a maximum at ~ 313 nm is weak compared with the lines at 395 nm and 466 nm, which indicates that $\text{NaGd}(\text{MoO}_4)_2:\text{Eu}^{3+}$ micro-powders are suitable for the nUV and blue LED chip. (b) For the nanocrystalline $\text{NaY}(\text{MoO}_4)_2:\text{Eu}^{3+}$ phosphor, its charge transfer band from O—Mo with a maximum at ~ 286 nm is very weak compared with the line at 466 nm, which indicates that the nanocrystalline $\text{NaY}(\text{MoO}_4)_2:\text{Eu}^{3+}$ phosphor is more suitable for the blue LED chip. For the $\text{NaY}(\text{MoO}_4)_2:\text{Eu}^{3+}$ micro-powders phosphor, its charge transfer band from O—Mo with a maximum at ~ 286 nm is very strong compared with the line at 466 nm. This different features between $\text{NaLn}(\text{MoO}_4)_2:\text{Eu}^{3+}$ ($\text{Ln} = \text{Gd}, \text{Y}$) micro-powders and nanocrystalline may be explained by the differences between the crystallite and size. It is possible that crystallite and size of the products have important effect on the luminescence of phosphors.

The emission spectra of Eu^{3+} (Fig. 3, right) excited under 466 nm are mainly dominated by the hypersensitive red emission, showing a strong transition $^5\text{D}_0 \rightarrow ^7\text{F}_2$ at 616 nm and a weak $^5\text{D}_0 \rightarrow ^7\text{F}_1$ transition. The two peaks are assigned to the electric dipole transition and magnetic dipole transition, respectively, and the presence of electric dipole transition confirms that Eu^{3+} ions are located at sites without inversion symmetry. Other transitions from the $^5\text{D}_0$ excited level to $^7\text{F}_j$ ground states are very weak, which is advantageous to obtain good Commission Internationale de l'Éclairage (CIE) chromaticity coordinates for phosphors. Therefore, they may be applied as a cheap and excellent red component for the fabrication of blue LED chip-based W-LEDs.

3.3. The High-Resolution $^7\text{F}_0 \rightarrow ^5\text{D}_0$ Excitation and Selectively Excited Emission Spectra

The electronic spectra of ions are broadened by various mechanisms. The broadening obscures features in the spectra, and can be especially problematic in making quantitative measurements in mixtures of energy levels. High-resolution laser spectroscopy of ions in crystals requires narrow-band width excitation sources that are only achievable with lasers. Studies in the visible spectral region typically use a tunable dye laser including the laser selective excitation experiments and high-resolution emission spectra.¹⁵ As far as we know, the Eu^{3+} ion is sensitive to the surrounding environment and the effect of the crystal field will cause shifts and splittings of crystal field levels. Therefore, the laser-selective excitation experiments and high-resolution emission spectra were performed for the as-synthesized samples to clarify the site occupation of Eu^{3+} doped in $\text{NaGd}(\text{MoO}_4)_2$ and $\text{NaY}(\text{MoO}_4)_2$.

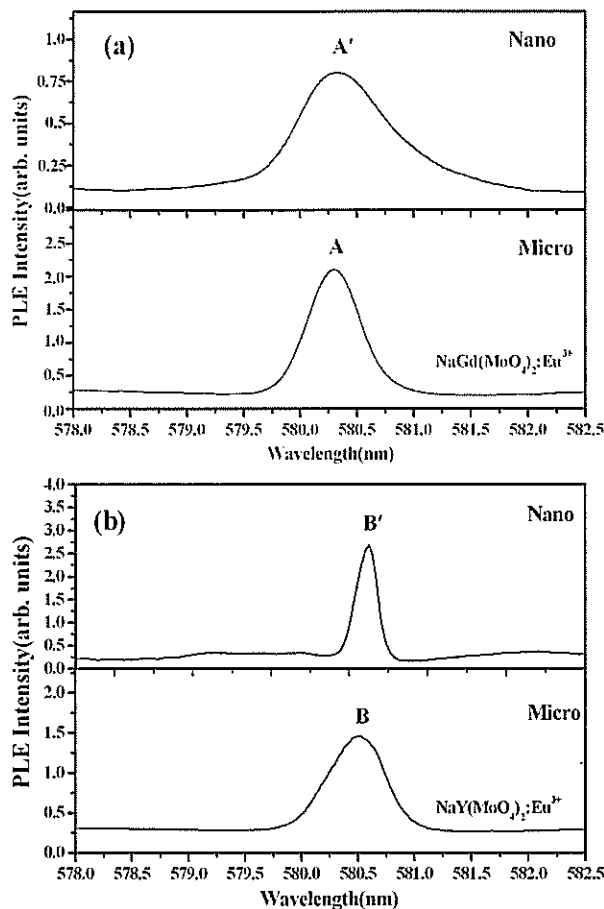


Figure 4. Site-selective photoluminescence excitation spectra of micro-powders and nanocrystalline $\text{NaGd}(\text{MoO}_4)_2:\text{Eu}^{3+}$ (a) and $\text{NaY}(\text{MoO}_4)_2:\text{Eu}^{3+}$ (b) phosphors measured by monitoring at 616.50 nm, respectively.

The laser-selective photoluminescence excitation spectra of $\text{NaLn}(\text{MoO}_4)_2:\text{Eu}^{3+}$ ($\text{Ln} = \text{Gd}, \text{Y}$) were measured by monitoring the $^5\text{D}_0 \rightarrow ^7\text{F}_2$ emission at 615.50 nm and displayed in Figures 4(a) and (b). It is well-known that the initial and final energy state involved in $^5\text{D}_0 \rightarrow ^7\text{F}_0$ transition is nondegenerate; only a single transition is expected. In this experiment, one line for $^7\text{F}_0 \rightarrow ^5\text{D}_0$ transition is recorded at 580.30 nm (site A), 580.33 nm (site A'), 580.50 nm (site B) and 580.50 nm (site B') for the $\text{NaLn}(\text{MoO}_4)_2:\text{Eu}^{3+}$ ($\text{Ln} = \text{Gd}, \text{Y}$) micro-powders and nanocrystalline, respectively, indicating that the Eu^{3+} ions occupy one crystallographic site of the Ln^{3+} ion. To our best knowledge, $\text{NaLn}(\text{MoO}_4)_2$ has a scheelite structure and space group centrosymmetric $I4_1/a$, which possesses a low symmetry lacking of inversion center. It is clear that Eu^{3+} ions displace the site of Ln^{3+} ions and are coordinated by eight O atoms in LnO_8 polyhedron site owing to their similar ion radius and valence. Figure 5 shows the highly resolved emission spectra of $\text{NaLn}(\text{MoO}_4)_2:\text{Eu}^{3+}$ ($\text{Ln} = \text{Gd}, \text{Y}$) upon excitation in the A, A', B and B' bands. One can observe that there is no distinct difference in the four emission spectra except for a little distinction of

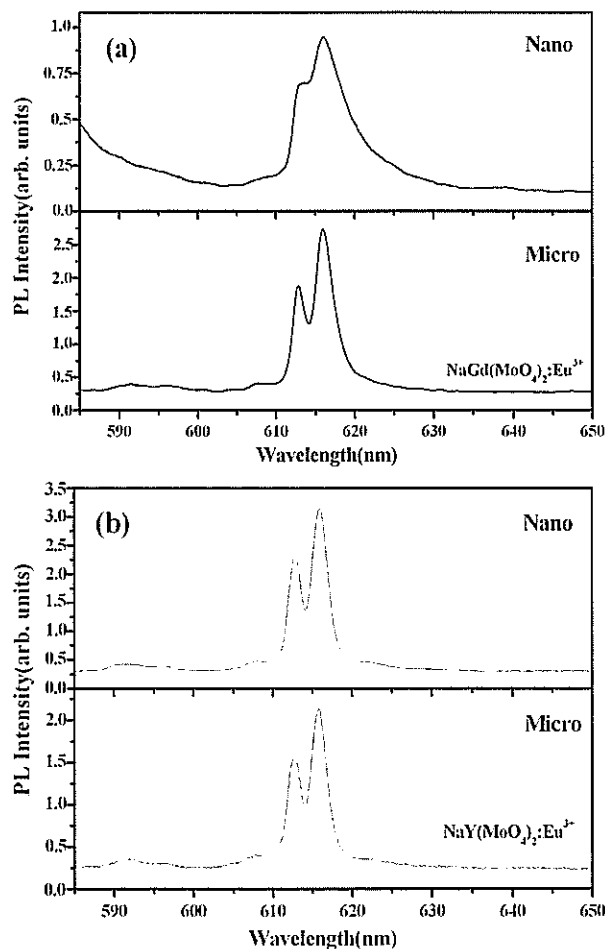


Figure 5. High-resolution emission spectra of micro-powders and nanocrystalline $\text{NaGd}(\text{MoO}_4)_2 \cdot \text{Eu}^{3+}$ (a) and $\text{NaY}(\text{MoO}_4)_2 \cdot \text{Eu}^{3+}$ (b) phosphors for the excitations at 580.30 nm (site A), 580.33 nm (site A'), 580.50 nm (site B) and 580.50 nm (site B'), respectively.

intensities. The $^5\text{D}_0 \rightarrow ^7\text{F}_2$ transition splits into three peaks confirming the existence of a single local low symmetry chemical environment for Eu^{3+} ion, which is compatible with a S_4 site symmetry.

In order to avoid the superimposition of images and signals, it is well known that the lifetime of phosphors applied in the field of displays and lights should be suitable.¹⁶ The photoluminescence decay curves of the as-obtained phosphors were also investigated. The decay curves of the $\text{NaLn}(\text{MoO}_4)_2$ ($\text{Ln} = \text{Gd}, \text{Y}$) doped with Eu^{3+} powders indicate that all the curves can be well fitted into a single exponential function as $I(t) = I_0 \exp(-t/\tau)$, where I is intensity, I_0 is initial intensity, and τ is decay lifetime. The lifetimes are determined to be 0.559 ms, 0.455 ms, 0.546 ms and 0.483 ms for $\text{NaY}(\text{MoO}_4)_2 \cdot \text{Eu}^{3+}$, Figure 6, micro-powders and nanocrystalline and $\text{NaGd}(\text{MoO}_4)_2 \cdot \text{Eu}^{3+}$ (not shown) samples, respectively. We found that the fluorescent lifetime of nanocrystal is shorter than that of micro-powders. It seems possible that the decrease in the lifetime when the particle

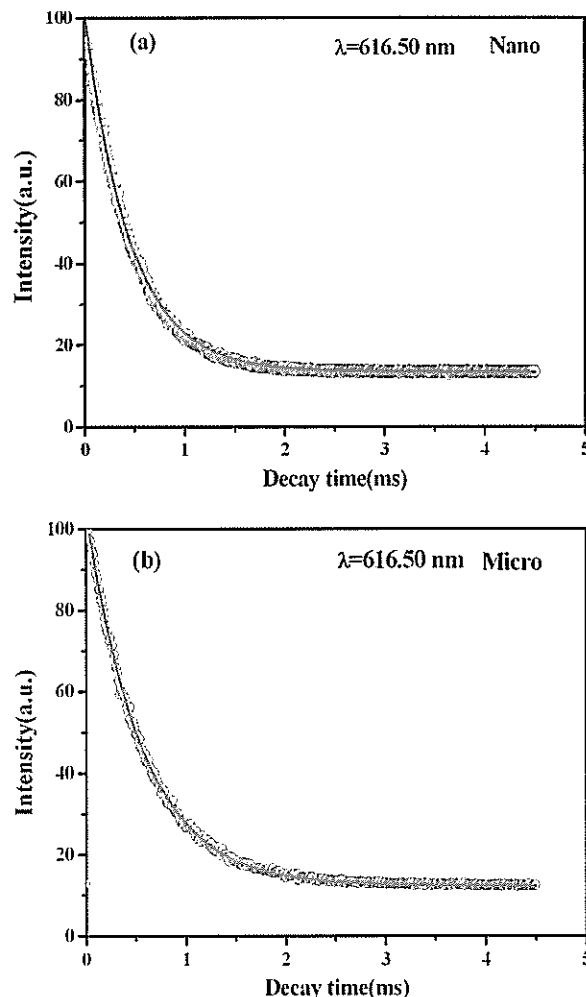


Figure 6. Decay curves for the as-prepared samples: (a) $\text{NaY}(\text{MoO}_4)_2 \cdot \text{Eu}^{3+}$ nanocrystalline (Round circles: experimental data; Red solid line: fitting results by $I = I_0 \exp(-t/\tau)$, $\tau = 0.455$ ms) and (b) $\text{NaY}(\text{MoO}_4)_2 \cdot \text{Eu}^{3+}$ micro-powders (Round circles: experimental data; Red solid line: fitting results by $I = I_0 \exp(-t/\tau)$, $\tau = 0.559$ ms).

size is decrease was probably due to the non-radiation relaxation caused by surface defects and hydrated species that act as quenching centers. The results show that the lifetime is short enough for potential applications in displays and lights.

4. CONCLUSION

From a detailed analysis of the site-selective laser excitation and emission spectroscopy in Eu^{3+} doped $\text{NaLn}(\text{MoO}_4)_2$ ($\text{R} = \text{Gd}, \text{Y}$), one crystallographic site in the $\text{NaLn}(\text{MoO}_4)_2$ is assigned. The luminescent properties of the $\text{NaLn}(\text{MoO}_4)_2 \cdot \text{Eu}^{3+}$ ($\text{Ln} = \text{Gd}, \text{Y}$) phosphors were investigated, showing strong absorption at 466 nm with a much intense red emission, which indicated that they might be applied as the cheap and excellent red component for the fabrication of blue LED chip-based W-LEDs. Further work is underway to study the luminescent properties

of better samples prepared by other methods and the possibility of synthesizing other related materials.

Acknowledgments: This work was supported by the National Science Foundation of China (no. 11004081), partially supported by the Science and Technology Innovation Projects of Jilin Province for overseas students and sponsored by Project 450091202144 Supported by Graduate Innovation Fund of Jilin University and by the Scientific Research Foundation for the Returned Overseas Chinese Scholars, State Education Ministry.

References and Notes

1. X. X. Zhao, X. J. Wang, B. J. Chen, Q. Y. Meng, B. Yan, and W. H. Di, *Opt. Mater.* 29, 1680 (2007).
2. F. Lei and B. J. Yan, *Solid State Chem.* 181, 855 (2008).
3. S. Neeraj, N. Kijima, and A. K. Cheethanl, *Chem. Phys. Lett.* 387, 2 (2004).
4. C. F. Guo, T. Chen, L. Luan, W. Zhang, and D. X. Huang, *J. Phys. Chem. Solids* 69, 1905 (2008).
5. S. M. Liu, W. Chen, and Z. G. Wang, *J. Nanosci. Nanotechnol.* 10, 1418 (2010).
6. S. K. Shi, M. Hossu, K. Jiang, and W. Chen, *J. Mater. Chem.* 22, 23461 (2012).
7. Y. F. Liu, W. Chen, S. P. Wang, and A. G. Joly, *Appl. Phys. Lett.* 92, 043901(2008).
8. Yu. K. Voron'ko, K. A. Subbotin, V. E. Shukshin, D. A. Lis, S. N. Ushakov, A. V. Popov, and E. V. Zharikov, *Opt. Mater.* 29, 246 (2006).
9. X. Z. Li, Z. B. Lin, L. Z. Zhang, and G. F. Wang, *J. Cryst. Growth* 29, 670(2006).
10. X. A. Lu, Z. Y. You, J. F. Li, Z. J. Zhu, G. H. Jia, B. C. Wu, and C. Y. Tu, *J. Alloys Compd.* 426, 352 (2006).
11. L. Macalik, J. Hanuza, J. Sokolnicki, and J. Legendziewicz, *Spectrochim. Acta A* 55, 251 (1999).
12. Z. L. Wang, H. B. Liang, M. L. Gong, and Q. Su, *Opt. Mater.* 29, 896 (2007).
13. M. Maczka, J. Hanuza, and A. Pietraszko, *J. Solid State Chem.* 154, 498 (2000).
14. V. A. Morozov, A. V. Arakcheeva, G. Chapuis, N. Guiblin, M. D. Rossell, and G. V. Tendeloo, *Chem. Mater.* 18, 4075 (2006).
15. P. M. Selzer, *Laser Spectroscopy of Solids*, Springer (1981).
16. G. Blasse and B. C. Grabmaier, *Luminescent Materials*, Springer, Berlin (1994).

Received: 15 August 2012. Accepted: 1 February 2013.